

Computation of Veils, Edge Detection Operators: Comparison with Wavelets Transform

Arunkumar H. M.¹ and Padmanabha Reddy A.^{2,*}

¹Research Scholar Department of Mathematics, VSK University, Ballari, Karnataka, India.

²Asst. Prof. Department of Mathematics, VSK University, Ballari, Karnataka, India.

Abstract

One of the important algorithms is an Edge detection operator is a beautiful application in many mathematical desires in real-world problems. This operator considerably reduces the quantity of data and filters out unwanted and it provides the many information within an image. the significant information is employed in a picture process to observe objects and there's some bad situation like false edge detection, issues due to noise, missing of low contrast boundaries in classical operators and therefore the scientifically don't understand specifically manner few optical illusions play tricks on human eyes. The wavelet transform has been shown that changed good edge operator provides a lot of accurate results for noise-free and noisy image respectively. The compared to other edge detection operators like classical operators Roberts, Prewitt, Sobel, LoG, and cagey with moving ridge remodel. Our contributions during this paper, the computed one dimensional for initial and second-order derivatives veils with the assistance of Taylor series. The computed veils are characteristic of a high frequency in signal or high intensity in pictures.

Keywords: Computing Veils, Canny Edge Detector, Automatics Threshold, Wavelets Transform, Edge Detection.

1. INTRODUCTION

Edge detection could be a procedure utilized in image process, mathematical, computer science and engineering desire applications. The fundamental objective of the edge detection is to identify discontinuities, singularity and particular items inside an image. These discontinuous and singularity in an image are as a result of fast changes in pixels intensity that distinguish boundaries objects during an encompassing. Edges provide boundaries between particular districts inside an image. These boundaries are utilized to understand objects [(Bhardwaj, & Mittal, A. (2012))]. The edge detectors are necessary for separating the edge. There is such an expansive number of edge identification operators accessible [(Main, R & Aggarwa, H.)] that can remove the edges from the noisy image, but the classical operators are edged gives less precise.

That's due to the nearness of clamor they extricate untrue edges. They don't find peculiarity and the boundaries of the object having little changes in force values but the result is destitute localization of edges. So the operator is required that see such an unfaltering alter in intensities and lost of moo contract boundaries, these operators seeing vertical, horizontal, flat, corner, step, ramp and roof edges, etc., the nature of edge recognized by these operators is high needy clamor, lighting conditions, objects same intensities. So expulsion of noise is required outcomes blurred and distorted edges in image/signal. Wavelet transforms is suitable for noisy images and gives remarkable performs.

In 1984, wavelet transform was presented by the French geophysicist Morlet to keep away from the bother or drawback of a transform with a fixed resolution in the spatial and frequency domains (Morlet and Grossmann, 1984) [(Deren L&Juliang, S. (1994))]. A while later, the commitments to the DWT (discrete wavelet transform) by Stromberg (1981) and Meyer (1985) caused wavelet transform empirical and particular images. Now a day, wavelets' developing the unused hypothesis is still being created hugely, and it developing additionally in the field's preferences engineering, physics, mathematics, and so on. quantum mechanics (Feberbush, 1987), (Daubechies, 1988), and signal processing (Martinet-Kronland and et al., 1990, Martin and Oliver, 1991), and so on. The canny arithmetic operator has been demonstrated to have great criminologist impact within the common utilization of edge detection. Be that as it may, Canny operator to has certain insufficiencies [(Wang, B & Fan, S. (2009))] this paper is motivated to us. This paper is organized as takes after in section 1 is a presentation. Section 2 presents an outline of related work for classical operators. In section 3 computing first and second-order derivative veils. In section 4 basic consideration of two dimensional. In section 6 choose threshold automatically. In section 6 edge detection based on wavelet transforms. In section 7 Empirical results and discussion. In section 8 performance matrices and section 9 conclusions.

* Corresponding Author: A. Padmanabha Reddy

2. CLASSICAL EDGE DETECTION OPERATORS

Different sorts of operators are accessible for edge detection [(Main, R & Aggarwa, H.)] however these operators are characterized into two classifications. 1) First-order derivative, 2) Second order derivative. In first-order derivative [(Bhardwaj, & Mittal, A. (2012))], the input is convolved with a balanced shroud to make a slope picture in which edges are the location. Most classical operators like Prewitt, Sobel, Roberts, and so on, [(Gonzalez, R. C., Woods, et al. (2016).)] are the first-order derivative operators, and these operators are moreover called as gradient operators. The slope operators identify edge by looking for most extraordinary force esteem, see at the circular of concentrated values within the neighborhood of a given pixel and choose whether the pixel is to be classified as an edge and can't be utilized in real-time applications.

In second-order derivative [(Main, R & Aggarwa, H.)] is depending on the extraction of zero-crossing centers which appears the closeness of maxima within the picture. The second-order derivative is amazingly delicate to noise, and the sifting functions are exceptionally imperative, the operators are determined from the Laplacian of Gaussian (LoG), proposed by Marr and Hildreth [(Marr, D & Hildreth, E. (1980))], the picture is smoothed by Gaussian filter. For this operator, we have to settle a number of parameters such as the fluctuation of the Gaussian channel. A noteworthy issue of LoG is that the localization of edges with a filter kernel profile by zero-crossing centers presents favoritism which increases with the smoothed effect of sifting.

2.1 Definitions of various edges

- 2.1.1 **Edge normal:** Unit vector toward most extreme intensity change.
- 2.1.2 **Edge direction:** Unit vector to opposite to the edge normal.
- 2.1.3 **Centre or Edge position:** The image position at which the edge is found.
- 2.1.4 **Edge strength:** Related to the local image contrast along the normal.

2.2. Edges modeled according to their intensity

- 2.2.1 **Step edge:** The image intensity quickly changes from one value to the other side of brokenness to an unmistakable value on the opposite side.
- 2.2.2 **Ramp edge:** A step edge where rapidly changes or not rapid but occur over a finite interval.
- 2.2.3 **Ridge edge:** The image intensity rapidly changes values but then returns to the starting values within

some short interval (produced by for the most part by lines).

- 2.2.4 **Roof edge:** A ridge edge where the intensity change is not rapid but occurs over a finite interval (created more often than not by the crossing point of surfaces).

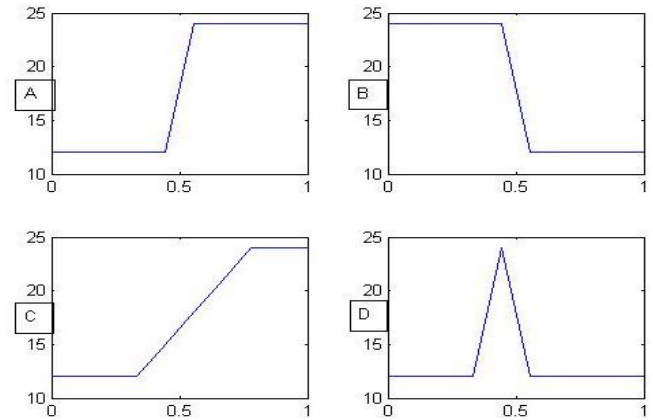


Fig. 1 A). Upward step edge, B). Downward step edge, C). Ridge edge D). Roof edge

3. COMPUTING FIRST AND SECOND-ORDER DEGREE DERIVATIVE VEILS USING TAYLOR SERIES FOR ONE DIMENSIONAL [(JAIN, R. K. & IYENGAR, S. R. K.. (2002))]:

3.1 First order degree of derivative veil

$$f(x+a) = f(x) + af'(x) + \frac{a^2}{2!}f''(x) + \frac{a^3}{3!}f'''(x) + \dots (1)$$

Where Eqn (1) is the Taylor series, and neglecting higher-order terms after first-order degree, it gives

$$f(x+a) \approx f(x) + af'(x),$$

$$f'(x) \approx \frac{f(x+a) - f(x)}{a}, \quad (2)$$

$$f'(x) \approx \frac{f(x) - f(x+a)}{a}, \quad (3)$$

Eqns (2) and (3) are forward and backward differences. Adding Eqns (2) and (3) we get central difference.

$$f'(x) \approx \frac{f(x+1) - f(x-1)}{2}.$$

Here $a = 1$, and $x, x+1, x-1$ denotes the present, forward and backward locations, finally we get veil using central difference $M = \left[\frac{1}{2}, 0, \frac{-1}{2} \right]$, here M is the first-order derivative veil.

3.2 Second-order degree of derivative veil

Using (1) is the Taylor series, and neglecting higher-order terms after second-order degree, it gives

$$f(x+a) \approx f(x) + af'(x) + \frac{a^2}{2!} f''(x),$$

$$\frac{a^2}{2!} f''(x) \approx f(x+a) - f(x) - af'(x), \quad (4)$$

We know that the first-order derivative of central difference is given by

$$f'(x) \approx \frac{f(x+a) - f(x-a)}{a}. \quad (5)$$

Eqn (3) put in eqn (4) and $a = 1$, we get

$$f''(x) \approx f(x+1) - 2f(x) + f(x-1), \quad (6)$$

Eqn (4) is called second-order degree derivative of central difference and gives the veil $M = [1, -2, 1]$. here M is the second derivative veil.

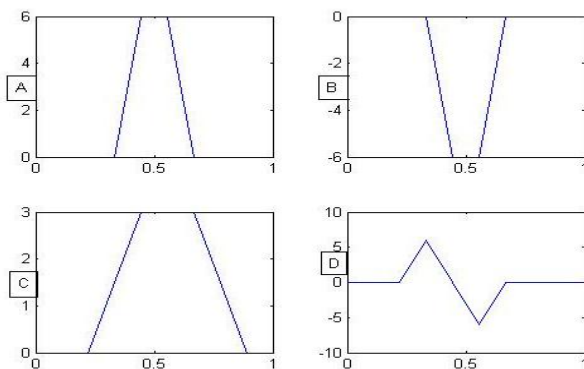


Fig. 2 TheFirst Derivative Veil, Convolution with Modeled Signals Respective A). Upward step edge, B). Downward step edge, C). Ridge edge D).Roof edge

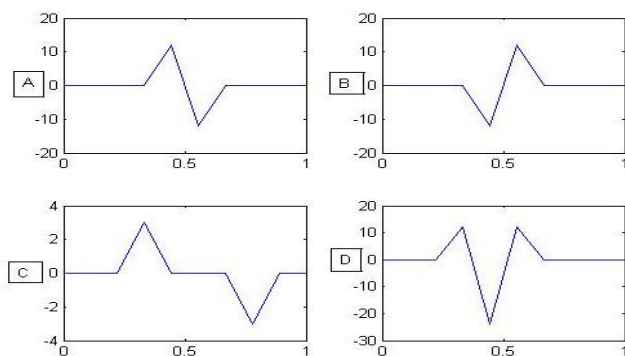


Fig. 3 The Second Derivative Veil Convolution with Modeled Signals Respective, A). Upward step edge, B). Downward step edge, C). Ridge edge D).Roof edge.

4. BASIC CONSIDERATION OF TWODIMENSIONAL

The display showing a white and black image at present contains a pixel spot of columns are rows. Each pixel spot is assigned by square co-ordinates, (x_1, y_1) , and decides a gray level value at the co-ordinates spot signify the darkness of gray. A digit grayscale picture is comprised of pixels. Routinely, the gray escalated of the pixels comprises of non-negative integrability extending from black (0) to white (255). We can ready perceive a gray level value at the co-ordinates spot signifies the darkness of the gray, will be assigned by $S(x_1, y_1)$. In any case, sometime recently we proceed with the edge location examination, we to begin with a survey a couple of basic variables based math and calculus ideas. We to begin with review the commonplace dab item for two vectors x and y to be $\langle x, y \rangle = \sum_{i=0}^2 x_i y_i$. From this dot or

inner product, we define the norm to be $\|x\| = \sqrt{\langle x, x \rangle}$ is exceptionally vital result to numerous applications that the cosine of the angle between the two vectors x and y , fulfil the

condition that $\cos(\theta) = \frac{\langle x, y \rangle}{\|x\| \|y\|}$, was each x and y is non-zero vectors. The most extreme esteem for the cosine happens when two vectors are coinciding giving esteem $\cos(0) = 1$, and the least esteem for the cosine happens when two vectors are orthogonal giving esteem $\cos\left(\frac{\pi}{2}\right) = 0$ [(Frazier, M. W.

(1999))]. These values are vital in edge detection. We presently present the halfway derivative formulas,

$$\frac{\partial S(x, y)}{\partial x} = \lim_{a_x \rightarrow 0} \frac{S(x+a_x, y) - S(x, y)}{a_x}, \quad (7)$$

and

$$\frac{\partial S(x, y)}{\partial y} = \lim_{a_y \rightarrow 0} \frac{S(x, y+a_y) - S(x, y)}{a_y}. \quad (8)$$

The separate between pixel areas will be normalized to be break-even with to one so all increases within the fractional derivative formulae will be rise to one. This gives,

$$\frac{\partial S(x, y)}{\partial x} \approx \frac{S(x+1, y) - S(x, y)}{1}, a_x = 1$$

and

$$\frac{\partial S(x, y)}{\partial y} \approx \frac{S(x, y+1) - S(x, y)}{1}, a_y = 1.$$

We presently indicate the work, $S(x, y)$ to be the gray balanced values between nearby pixels within the horizontal and vertical bearings, separately, giving us the formulas $S(x_1 + 1, y_1) - S(x_1, y_1)$. $S(x_1, y_1 + 1) - S(x_1, y_1)$. The extraordinary locations, x_1 and y_1 can as it took on integer values gifted by their pixel locations [(Schmeelk, J. (2005))].

5. CHOOSE BEST THRESHOLD VALUE AUTOMATICALLY [(GONZALEZ, R. C. ET AL. (2016))]

In most cases in image processing, the favorite approach is to use an operator is able to perform of choosing a threshold automatically based on image data. The following iterative procedure is such approach:

- i. Select an initial guess value for the global threshold (Thr)
- ii. Segment the image utilizing Thr . This will outcome two groups of pixels S_1 exist of all pixels along intensity values greater than Thr and S_2 exist of pixels along values less than or equal to Thr .
- iii. Calculate the average intensity values m_1 and m_2 for the pixels in domain S_1 and S_2 respectively.
- iv. Calculate a new threshold value

$$Thr = \frac{m_1 + m_2}{2}$$

- v. Repeat step 2 done four units the distinctness in Thr in flowing iterations is smaller than a predefined value.
- vi. Segment the image using MATLAB functions `im2bw` (8-bit image) that scales the highest value of ratio threshold divided by highest number (255) to one.

6. EDGE DETECTION BASED ON WAVELET TRANSFORMS

The wavelet hypothesis has permitted a few earlier in tolerating of multi-scale edges. It has been appearing [(Grossman A & Morlet, J. (1984)), (Mallat, S & Hwang, W. L. (1992))] that multi-scale edges can be recognized from the maxima focuses of the wavelet transforms modulo of a image. Presently a day colossally utilized edge discovery hypothesis based on Canny's method [(Canny, J)]. It interfaces a smoothing step employing a low-pass filter of a certain width and a separation step. Smoothing some time recently calculating the angle of the gray level work related inside a picture is ordained to reduce noise effect and to supply regularization of the computerized picture. Edge focuses are at

that point decided as focuses where the modulus of the slope vector is locally most extreme within the direction towards which the slope vector focuses in a picture plane. A gradient operation gotten from the separation of the smoothing filter permits the combination of the two steps [(Canny, J)], the measure of the smoothing filter characterizes the analyzing scale of the image. Let us define the Gaussian filter at scale α :

$$S_\alpha(x, y) = \frac{1}{2\pi\alpha^2} e^{-\frac{1}{2\alpha^2}(x^2+y^2)}, \quad (9)$$

The associated gradient operator $\nabla S_\alpha(x, y) = \begin{pmatrix} \frac{\partial S(x, y)}{\partial x} \\ \frac{\partial S(x, y)}{\partial y} \end{pmatrix}$, using

Eqns (7) and (8) as providing in [(Schmeelk, J. (2005))], the gradient operator is break even with to the continuous wavelet transform calculated with a wavelet determined from the gradient of a Gaussian function and characterized as:

$$\Psi_\alpha(x, y) = \begin{pmatrix} \Psi_\alpha^1(x, y) \\ \Psi_\alpha^2(x, y) \end{pmatrix} = \alpha \begin{pmatrix} \frac{\partial S(x, y)}{\partial x} \\ \frac{\partial S(x, y)}{\partial y} \end{pmatrix}, \quad (10)$$

The associated continuous transforms $WS(\alpha, x, y)$ of a function $S(x, y)$ is then

$$WS(\alpha, x, y) = \begin{pmatrix} W^1 S(\alpha, x, y) \\ W^2 S(\alpha, x, y) \end{pmatrix} = S * \Psi_\alpha(x, y) \quad (11)$$

Here, * represents the convolution product. The characterized vector wavelet transform can be considered to be a wavelet transform gotten through a wavelet Ψ_α defined as

$$\Psi_\alpha = \Psi_\alpha^1 + \Psi_\alpha^2, \quad (12)$$

Edges can be identified from the modulus neighborhood maxima of the over wavelet transform, within the course demonstrated by the contention of this wavelet transform.

The proposed method can be divided into the following steps are given:

- i. Consider the standard image and addition Speckle noise to the original images.
- ii. Mathematically defined as:

$$S = z + y_n.$$

Where z is the original image, y_n is noise i.e., Speckle noise.

- iii. Apply threshold

- iv. The noisy image (S), S is decomposed into first levels based on the wavelets transform for Doubechies2 (db2).
- v. Finally Detected boundary of edges.

transforms the accuracy of positioning boundaries and provides a better and evident de-noising effect. In this paper we are shown only original images with noise added and after empirical results are shown only noisy edge detections figures.

7. EMPIRICAL RESULTS AND DISCUSSION

Four images are used in this empirical for analysis. These are standard images like's vegetables, coins and polygons with respective fig4 A, B, and C with Speckle noise contained 0.001 in the images fig4 D, E and F. One of them is optical illusion image as shown in figure 8 and below section. From the result of the location, the wavelet transforms features a way better detection impact, compared with classical operators likes Robert, Prewitt, Sobel, LoG and Canny as shows below figures from 5 to 7 respectively. These operators detect fewer edges boundaries as shown in figures 5 to 7 especially on the vegetables, coins and polygons boundaries are discontinuous as well as not clear visible compare to the wavelet transform. Their performances are analyzed concerning visualization and ratio edge pixels of size (REPS(%)) [(Prasad, P. M. K., et al (2016))], as shown below figures and table 1. This experiment demonstrates that wavelet

7.1 Optical Figment Image

A visual figment moreover called as optical figment is speaking to by outwardly seen pictures that unmistakable from the genuine question. Optical figments are intriguing visual marvels. Here is a surprising collection of nippy figments that will dumbfound your intellect. Numerous of these figment pictures can keep you locked in for hours. The report collected by the eye is prepared and the brain to provide a statute that does not count with a physical estimation of the boost source. Underneath figure 8 are optical figments that will trap your eyes. The pictures appear (in fig 8) to be legs are even confused though they are really how many legs. This is an example of our eyes relaying information to the brain and not being able to clearly identify exactly what it is what we see through our conscious awareness.

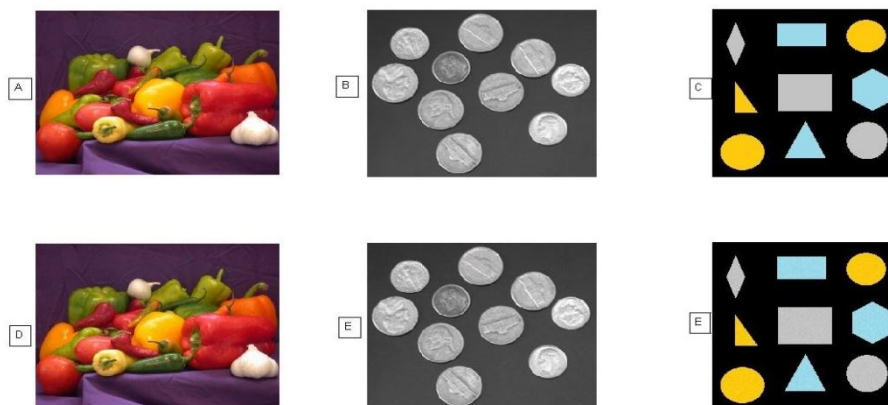


Fig. 4 Considered noiseless and noisy image of A) Vegetables, B) Coins and C) Polygons are original images. D), E), and F) are noisy image with Speckle noise 0.001.

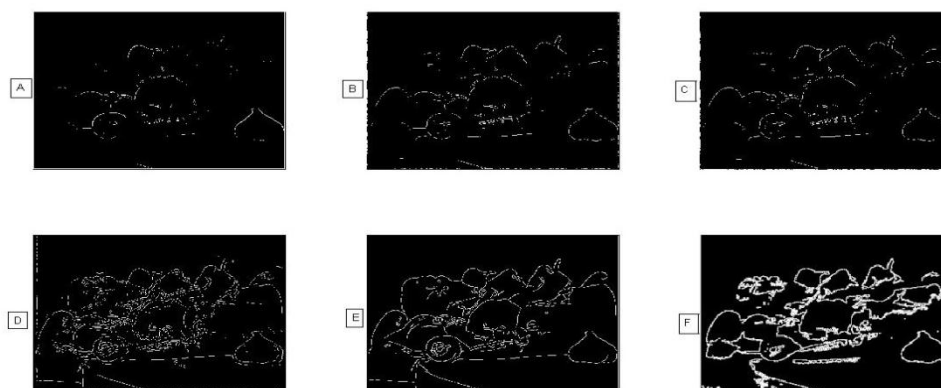


Fig. 5 Detected boundary edges of the Speckle noisy vegetable image by various operators, A). Roberts Operator, B). Prewitt Operator, C). Sobel Operator, D). Laplacian Operator (LoG), E). Canny Operator, F). Wavelet Transform.

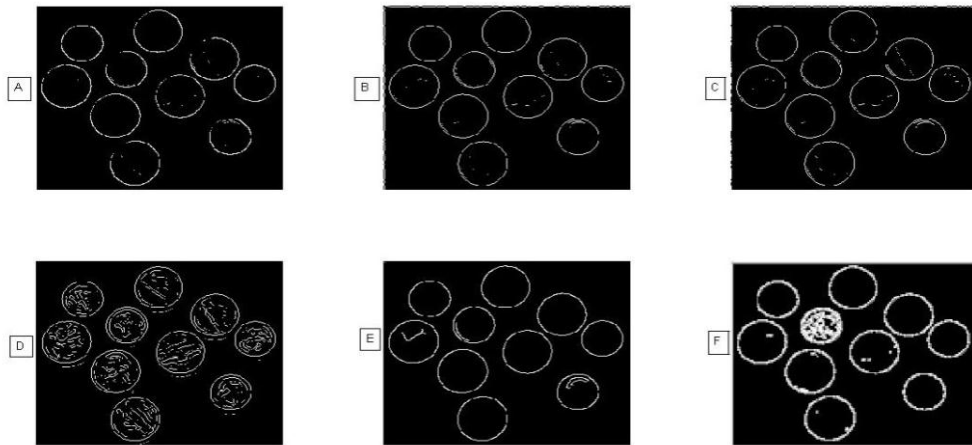


Fig. 6 Detected boundary edges of the noisy coins image by various operators, A). Roberts operator, B). Prewitt operator, C). Sobel operator, D). Laplacian operator (LoG), E). Canny operator, F). Wavelet transform.

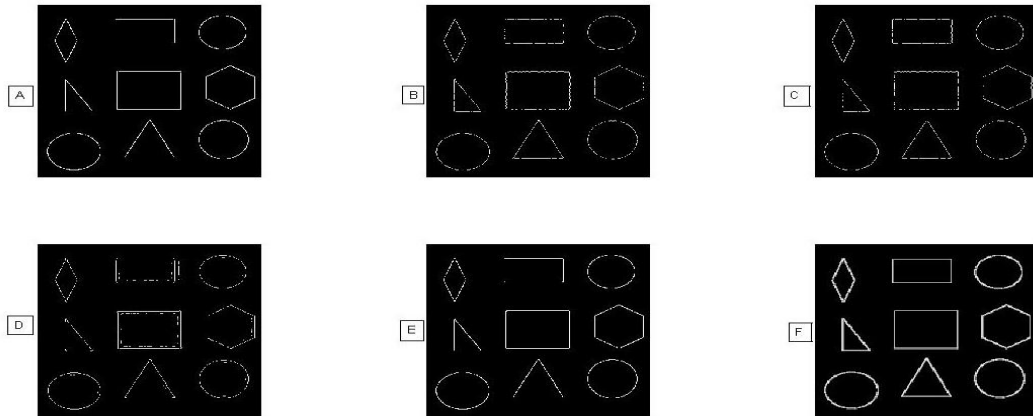


Fig. 7 Detected boundary edges of the noisy polygons image by various operators, A). Roberts Operator, B). Prewitt Operator, C). Sobel Operator, D). Laplacian Operator (LoG), E). Canny Operator, F). Wavelet Transform.

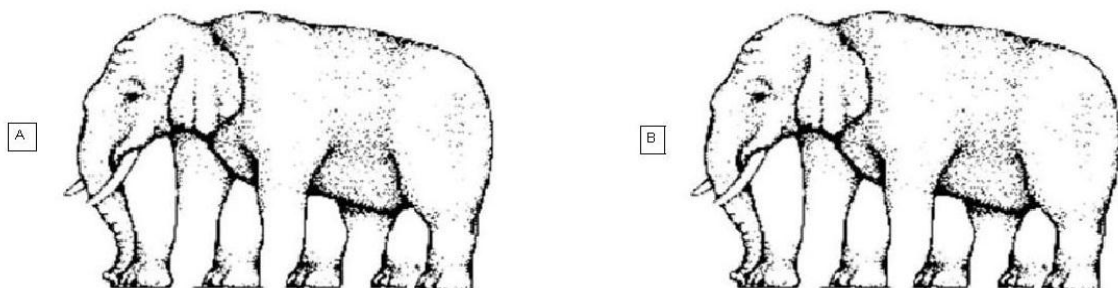


Fig. 8 Considered optical illusion elephant image. We may or may not find properly elephant legs from left to right, A) Original optical illusion image, B) Speckle noise added with 0.01 images.

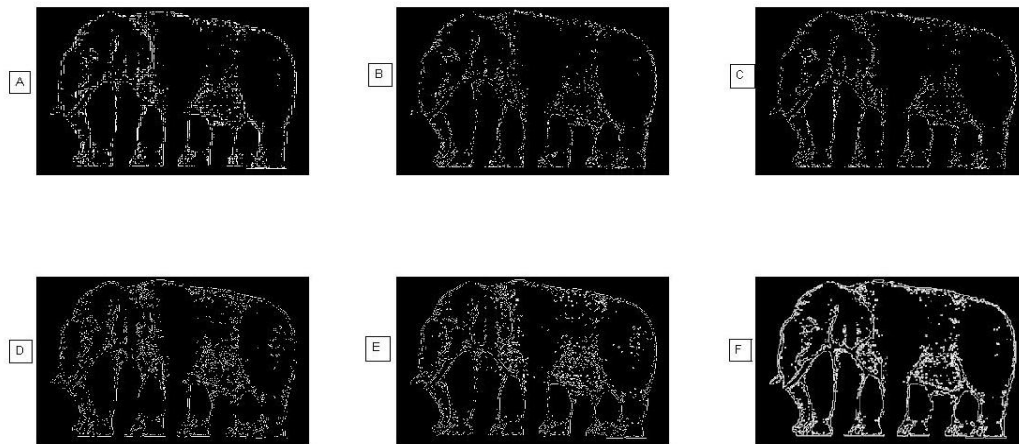


Fig. 9 After detected boundary edges of the noise free optical illusion image by various operators, A). Roberts operator, B). Prewitt operator, C). Sobel operator, D). Laplacian operator, may be clear visible of elephant legs (LoG), E). Canny operator, F). Wavelet transform.

Table 1. Performances of ratio edge pixels of size image (REPS) for various edge detection operators with noiseless and noisy images

Various Edge Operators	Vegetable Image REPS (%)		Coins Image REPS (%)		Polygons Image REPS (%)		Optical Figment Elephant	
	Noise free	Noisy	Noise free	Noisy	Noise free	Noisy	Noise free	Noisy
Roberts	1.3376	1.3426	3.1585	3.1598	5.3687	5.3649	4.9958	4.8962
Prewitt	1.7189	1.7264	3.0328	3.0423	4.2365	4.2099	3.6463	3.6692
Sobel	1.7717	1.7828	3.0956	3.1033	4.2422	4.2251	3.6598	3.6779
LoG	3.9886	4.0057	4.9167	4.8839	4.4550	4.8330	5.1080	5.0462
Canny	3.6762	3.7074	2.8347	2.8429	5.3383	5.3251	5.6861	5.6538
Wavelet Transform	8.5019	8.6891	9.7131	9.7172	22.1931	22.1931	24.1953	24.2246

Note: This Table contains classical operators and constructed with the help of MATALB inbuilt functions comparison with wavelet transform. Threshold values selected automatically based on data for Wavelet Transform (WT) mentioned in section 6 above and for Canny operator having Threshold value is mean of original image and divided by 255. i.e., 255 is highest value in 8-bit image.

9. PERFORMANCE METRICS

- i. Visual impacts: The quality of an picture is subjective and relative, depending on the perception of the client.
- ii. Ratio edge pixels of size image (REPS): if the pixel value of the image or edge point [(Prasad, P. M. K., et al. (2016.))].

$$REPS(\%) = \frac{\text{number of edge pixels}}{\text{size of an image}} \times 100$$

10. CONCLUSIONS

Since edge detection is the initial step in object recognition, it is important to know the differences between edge detection operators. In this paper, we studied the most commonly used edge detection operators of first derivative-based edge detection. First, derivative-based operators such as the Roberts, Prewitt and Sobel and second-order derivative such as Laplacian of Gaussian filters have a major drawback of being very sensitive to noise and drawback of Canny operator false zero-crossing with sensitivity to noise.

The classical operator's size of the kernel filter and coefficients are fixed and cannot be adapted to a given image. In the wavelet transforms considered the whole image. The performance of the wavelet transforms on the adjustable automatic threshold values controls the visible of edge detection boundaries and better ratio edge pixels of size image (RESP (%)) compare to the classical operators as shown above table 1. One more special image in this paper that is optical illusion image, before transform quite confused to counts legs of the elephant, after transform is probably is not taking too much time and it easily counts. But it may be contains fewer noise and slightly blurred edges, this paper supports a Speckles noise.

ACKNOWLEDGMENT

The first author acknowledges the department of studies in mathematics and Sc/St cell of Vijayanagara Sri Krishnadevaraya University, Ballari towards the funding for the research.

REFERENCES

- [1]. Bhardwaj, S., and Mittal, A., 2012, "A Survey on Various Edge Detector Techniques," *Procedia Technology*, 2012, pp 220 –226.
- [2]. Canny, J., 1986, "A Computational Approach to Edge Detection," *IEEE Transaction on Pattern Analysis and Machine Intelligence*, pp. 679-698.
- [3]. Deren, L., and Juliang, S., 1994, "The Wavelet and its Application in Image Edge Detection," *ISPRS Journal of Photogrammetry and Remote Sensing*, 49, pp. 4-11.
- [4]. Frazier, M. W., 1999, "An Introduction to Wavelets through Linear Algebra," Springer New York, pp.79-82.
- [5]. Gonzalez, R. C., Woods, R. E., and Eddins, S. L., 2016, "Digital Image Processing using Matlab," McGraw Hill, pp. 495-513.
- [6]. Grossman, A., and Morlet, J., 1984, "Decomposition of Hardy Functions into Square Integrable Wavelets of Constant Shape," *SIAM J*, pp.723-736.
- [7]. Jain, R. K., and Iyengar, S. R. K., 2002, "Advanced Engineering Mathematics," Norasa, 1sted, pp. 19.
- [8]. Main, R., and Aggarwa, H., "Study and Comparison of Various Image Edge Detection Techniques," *International Journal of Image Processing*, 3(1). pp. 1-12.
- [9]. Mallat, S., and Hwang, W. L., 1992, "Singularity Detection and Processing with Wavelets," *IEEE Transactions on Information Theory*, 38, pp.617-643.
- [10]. Marr, D., and Hildreth, E., 1980, "Theory of Edge Detection," *Proc. R. Soc. Lond. B* 207, pp.187-217.
- [11]. Prasad, P. M. K., Prasad, D. Y. V., and Sasibhushana R. G., 2016, "Performance Analysis of Orthogonal and Bio-Orthogonal Wavelets for Edge Detection of X-Ray Images," *Procedia Computer Science*, pp. 116 – 121.
- [12]. Schmeelk, J., 2005, "Wavelet Transforms and Edge Detectors on Digital Images," *Mathematical and Computer Modelling* vol. 41, pp. 1469-1478.
- [13]. Wang, B., and Fan, S., 2009, "An improved CANNY edge detection algorithm," *IEEE, Computer Society*, pp. 497-500.